

Non-meanfield deterministic limits in chemical reaction kinetics

R. E. Lee DeVille

Courant Institute of Mathematical Sciences, New York University, New York, New York 10012

Cyrill B. Muratov

Department of Mathematical Sciences, New Jersey Institute of Technology, Newark, New Jersey 07102

Eric Vanden-Eijnden

Courant Institute of Mathematical Sciences, New York University, New York, New York 10012

(Received 21 April 2006; accepted 30 May 2006; published online 20 June 2006)

A general mechanism is proposed by which small intrinsic fluctuations in a system far from equilibrium can result in nearly deterministic dynamical behaviors which are markedly distinct from those realized in the meanfield limit. The mechanism is demonstrated for the kinetic Monte Carlo version of the Schnakenberg reaction where we identified a scaling limit in which the global deterministic bifurcation picture is fundamentally altered by fluctuations. Numerical simulations of the model are found to be in quantitative agreement with theoretical predictions. © 2006 American Institute of Physics. [DOI: 10.1063/1.2217013]

It is well-known that despite the presence of intrinsic fluctuations, the dynamics of many microscopic systems may be captured by deterministic equations of motion when the system size is sufficiently large.¹⁻³ This is the so-called meanfield limit, and it is at the very heart of the majority of macroscopic models of physical, chemical, and biological systems. In this limit, fluctuations decouple from the volume-averaged quantities and manifest themselves as small irrelevant noise on top of a completely deterministic motion.

However, as was recently shown, these meanfield models can be non-robust with respect to small random perturbations in the presence of multiple dynamical time scales.⁴⁻⁹ This occurs when the time scale of the slow components in the dynamics matches that of the rare noise-activated barrier crossing events^{2,3,10-12} acting on the fast components. Surprisingly, this interplay can create new behaviors which are dramatically different from those in the meanfield limit and yet remain *deterministic* in the small noise limit. This puts into question the general applicability of the meanfield models for the study of the coherent dynamics in systems with underlying randomness. An important class of such microscopic systems are kinetic Monte Carlo (KMC) schemes^{13,14} for chemical and biochemical reactions,¹⁵⁻¹⁸ in which randomness is due to the underlying stochastic jump processes.² Here the meanfield (or extensive) limit results in the deterministic equations for concentrations of the reacting species (the mass action law).

In this paper, we show that the non-trivial interplay between rare events and slow dynamics leading to breakdown of the meanfield description is possible in systems far from equilibrium with intrinsic randomness. We do so by identifying distinguished *non-meanfield limits* in which the dynamics of the system is completely deterministic and at the same time remains distinct from the one governed by the mass action law. Existence of such limits implies existence of large regions in the parameter space where the predicted

phenomena can be robustly observed. We first explain the proposed mechanism by means of a general model, and then demonstrate it to be feasible in a specific example of an autocatalytic reaction KMC scheme.

Our general model is a “drift-or-jump” dynamical system whose state at any moment is described by a vector $y \in \mathbb{R}^m$. During an infinitesimal time interval dt the system will move by $dy = g_\alpha(y)dt$ to a new location $y + dy$, or jump instantaneously to a new position $p(y) \in \mathbb{R}^m$ with probability $k_\varepsilon(y)dt$. Here $g_\alpha(y)$ is a given vector field, $k_\varepsilon(y)$ is a jump rate, and $p(y)$ is a mapping which, for simplicity, we will assume to be one-to-one. The Chapman-Kolmogorov equation for the probability density $\rho(y, t)$ of this Markov process is²

$$\frac{\partial}{\partial t} \rho(y, t) = - \frac{\partial}{\partial y} (g_\alpha(y) \rho(y, t)) - k_\varepsilon(y) \rho(y, t) + k_\varepsilon(p^{-1}(y)) \rho(p^{-1}(y), t). \quad (1)$$

In the following, we are interested in a particular situation in which the drift is “slow” and the jumps are “rare,” quantified by two small dimensionless parameters, α and ε , respectively. More precisely, we assume that

$$g_\alpha(y) = \alpha g(y), \quad k_\varepsilon(y) = \nu(y) \exp\{-\varepsilon^{-1} V(y)\}, \quad (2)$$

i.e., α characterizes the slow time scale of the drift generated by g_α relative to some reference $O(1)$ time scale, and ε is the intensity of the jumps. Importantly, we assumed that the rate $k_\varepsilon(y)$ is in Arrhenius form, with $V(y)$ playing the role of a “barrier height” to be crossed in the event of a jump and $\nu(y)$ being a dimensional rate prefactor assumed to be $O(1)$ on the reference time scale.

If we let $\varepsilon \rightarrow 0$ in Eq. (1) with all other parameters fixed, then the last two terms in Eq. (1) disappear, and the limiting dynamics reduces to the deterministic motion $\dot{y} = \alpha g(y)$, the meanfield limit. However, as we show now, more interesting behaviors occur if we let $\varepsilon \rightarrow 0$ and $\alpha \rightarrow 0$ simultaneously on

some specific sequence and make some extra assumptions. For instance, suppose that (i) the map $p(y)$ satisfies $\forall y \in \mathbb{R}^m: V(p(y)) > V(y)$ (i.e., y always jumps to a state where the jump rate is smaller), and (ii) $\forall y \in \mathbb{R}^m: \nabla V(y) \cdot g(y) < 0$ (i.e., the deterministic drift drives the system toward regions of higher jump rate). Rescale time and introduce β as

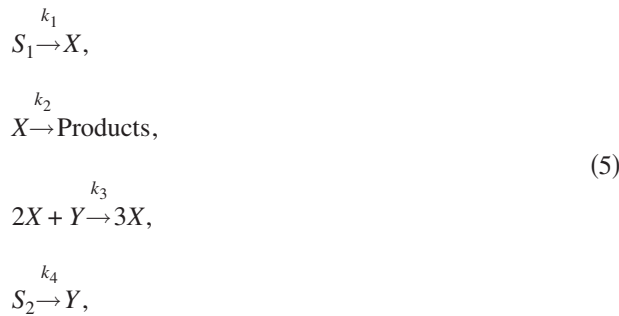
$$\tau = \alpha t, \quad \beta = \varepsilon \ln \alpha^{-1}, \quad (3)$$

and observe that in Eq. (1) written in the new time scale the jump rate is $k(y) \equiv \alpha^{-1} k_\varepsilon(y) = \nu(y) \exp\{\varepsilon^{-1}(\beta - V(y))\}$. Therefore, if we let $\alpha, \varepsilon \rightarrow 0$ in a way that $\beta = O(1)$ is kept fixed, then

$$k(y) \rightarrow \begin{cases} 0, & y \in \Omega_\beta, \\ \infty, & y \notin \bar{\Omega}_\beta, \end{cases} \quad (4)$$

where $\Omega_\beta \subset \mathbb{R}^m$ is the region where $V(y) > \beta$. So the following will happen: Supposing that the system starts from $y \in \Omega_\beta$, it will drift deterministically toward the boundary of this region, $\partial\Omega_\beta$, where $V(y) = \beta$. Once it reaches $\partial\Omega_\beta$, an instantaneous jump will occur to a new location $p(y) \in \Omega_\beta$, and the process will repeat itself indefinitely by the assumption above. The resulting dynamics in this limit is deterministic (since both the drift and the jump outcome are prescribed), but it is *strongly* non-meanfield, since it is very different from the solution of $dy/d\tau = g(y)$. This new non-meanfield deterministic behavior was termed self-induced stochastic resonance (SISR) in Refs. 8 and 9 (see also Ref. 7). We also note that for small but finite α, ε these dynamics should be augmented by a boundary layer analysis of Eq. (1) near $\partial\Omega_\beta$.

In the model above we postulated Eq. (1) and made some specific assumptions about the terms in this equation. Next we show that this equation can in fact be *derived* in a particular example in which it is not *a priori* obvious. We take the KMC scheme for the Schnakenberg reaction:¹⁹



which is a classical autocatalytic reaction scheme exhibiting limit cycle oscillations and capturing a number of essential non-equilibrium features of more realistic chemical and biochemical reactions (see, e.g., Ref. 20).

In the KMC version of the Schnakenberg reaction the state of the system at any time is given by the pair (X, Y) of integers corresponding to the numbers of molecules of the respective species. To identify the fast/slow dynamics, we first introduce the rescaling (we absorb S_1 and S_2 into the rate constants)

$$x = k_1^{-1} X, \quad y = (k_3 k_1^2 / k_4) Y, \quad (6)$$

and the dimensionless quantities

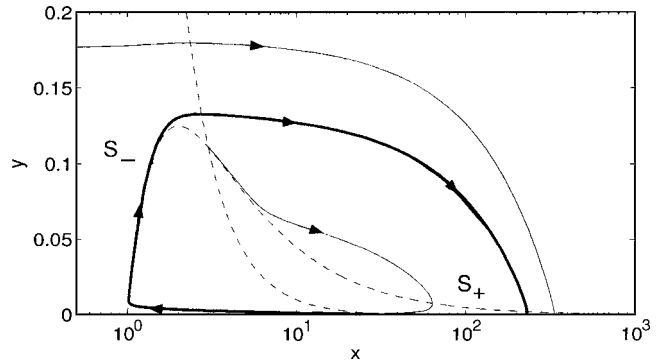


FIG. 1. Phase plane trajectories for Eq. (9) with $A=2$ and $\alpha=10^{-3}$. The limit cycle is indicated with a solid loop.

$$\alpha = k_1^2 k_3 / k_2^3, \quad \varepsilon = k_2 / k_1, \quad A = k_4 / k_1. \quad (7)$$

After rescaling, the Chapman-Kolmogorov equation for the probability density function $\rho(x, y, t)$, where $(x, y) \in \varepsilon \mathbb{Z}_+ \times (\varepsilon \alpha / A) \mathbb{Z}_+$, of this Markov process is

$$\begin{aligned} \frac{\partial \rho(x, y, t)}{\partial t} = & \varepsilon^{-1} [\rho(x - \varepsilon, y, t) - \rho(x, y, t) \\ & + (x + \varepsilon) \rho(x + \varepsilon, y, t) - x \rho(x, y, t) \\ & + A(x - \varepsilon)(x - 2\varepsilon) \rho(x, y, t) \\ & \times \rho(x - \varepsilon, y + \varepsilon \alpha / A, t) - A x(x - \varepsilon) y \rho(x, y, t) \\ & + A \rho(x, y - \varepsilon \alpha / A, t) - A \rho(x, y, t)]. \end{aligned} \quad (8)$$

Taking the limit $\varepsilon \rightarrow 0$ in Eq. (8) with all other parameters fixed, we obtain the deterministic process described by the mass action law (the meanfield limit):

$$\dot{x} = 1 - x + A x^2 y, \quad (9)$$

$$\dot{y} = \alpha(1 - x^2 y),$$

where now we measure time in the units of k_2^{-1} . From this, one can see that the constant α measures the time scale separation ratio between x and y , and the constant A controls the location of the unique fixed point

$$x_0 = 1 + A, \quad y_0 = (1 + A)^{-2}. \quad (10)$$

For α , small enough Eq. (9) exhibits a limit cycle when $A > 1$, i.e., when the fixed point (x_0, y_0) lies on the unstable branch S_+ , where $x = x_+(y)$,

$$x_{\pm}(y) = (1 \pm \sqrt{1 - 4Ay}) / (2Ay), \quad (11)$$

of the x -nullcline (Fig. 1). In contrast, there is no limit cycle when $A < 1$. In this case the fixed point lies on the stable branch S_- , where $x = x_-(y)$, of the nullcline and this fixed point is stable and globally attracting. During the slow motion, x remains close to $x_-(y)$, and so to leading order in $\alpha \ll 1$, y satisfies $\dot{y} = \alpha g(y)$ with

$$g(y) = 1 - x_-^2(y) y.$$

Now we turn to the analysis of the model for $\alpha, \varepsilon \ll 1$ with $\beta = O(1)$, following the general discussion earlier and show that a non-meanfield deterministic behavior emerges in this case. To obtain the transition rate $k_\varepsilon(y)$, we need to con-

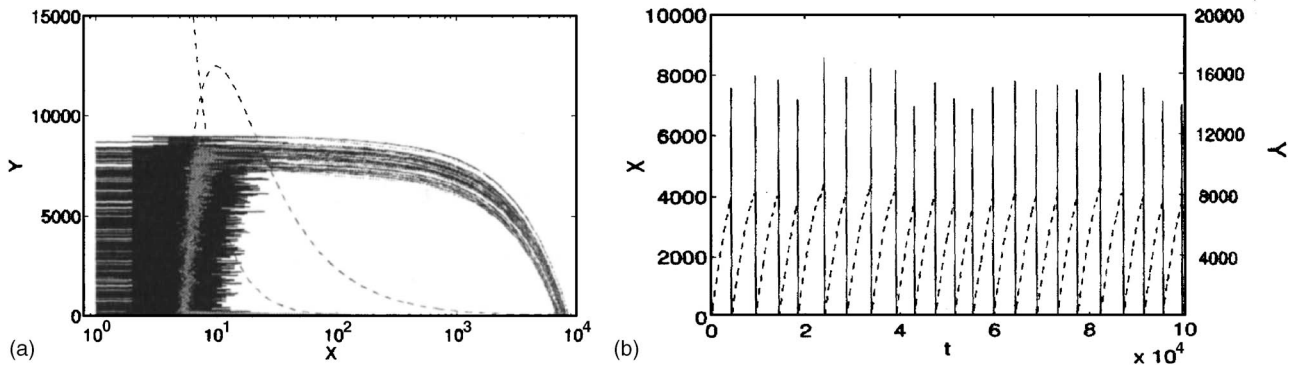


FIG. 2. Results of the KMC simulation of Eq. (5), with $k_1=5$, $k_2=1$, $k_3=4 \times 10^{-6}$, and $k_4=2.5$. In (a) we plot a sample trajectory in (X, Y) -space in black. Over this we have plotted in gray the running average over 1000 steps of the simulation, to show the typical size of the fluctuation (the fluctuations in the raw trajectory are exaggerated by rare large deviations). In (b) we plot X and Y vs time.

sider the escapes from the vicinity of S_- with y frozen. Setting $\alpha=0$ in Eq. (8), one sees that this amounts to studying a one-dimensional jump process in x with right and left jump rates:

$$\lambda_\varepsilon^+(x) = 1 + Ax(x - \varepsilon)y, \quad \lambda_\varepsilon^-(x) = x. \quad (12)$$

For $\varepsilon \ll 1$ the trajectory needs to reach S_+ in order to escape from the neighborhood of S_- . The corresponding rate of this escape event gives the $k_\varepsilon(y)$ to use in the equivalent of Eq. (1), and it can be determined by generalizing the classical analysis of Kramers² for the one-dimensional jump process with rates from Eq. (12).²¹ This gives an expression for $k_\varepsilon(y)$ which is in the form of Eq. (2) where (see also Ref. 3)

$$V(y) = \int_{x_-(y)}^{x_+(y)} \ln \left(\frac{\lambda_0^-(x)}{\lambda_0^+(x)} \right) dx \quad (13)$$

and

$$\nu(y) = \frac{2Ay\sqrt{1-4Ay}}{\pi(1+\sqrt{1-4Ay})^2}. \quad (14)$$

The function $V(y)$ in Eq. (13) can be easily computed in closed form. In particular, $V(y)$ is a monotonically decreasing function of y for fixed A . It follows that, given any $\beta > \beta_c(A) = V(y_0)$, we have $\beta = V(y_*)$ for some $y_* = y_*(\beta, A)$ with $0 < y_* < y_0$. As a result, in the limit $\alpha, \varepsilon \rightarrow 0$ with $\beta > \beta_c(A)$ fixed, the trajectory will jump precisely at $y = y_*$ consistent with Eq. (4) (here $\Omega_\beta = \{y < y_*\}$ and $\partial\Omega_\beta = \{y_*\}$).

After escape the process undergoes an excursion governed by Eq. (9) (instantaneous on the current time-scale), similar to the one considered in Ref. 8, after which it returns to S_- at $p(y) = 0$. Thus, the non-meanfield behavior predicted from Eq. (1) precisely arises in the present example and is an instance of SISR due to intrinsic noise. The observed non-meanfield behavior is a limit cycle with period (in units of α^{-1})

$$T(A, \beta) = \int_0^{y_*} \frac{dy}{g(y)}, \quad (15)$$

which is controlled by β .

For small but finite α and ε the escape region will be smeared. To compute the deviations from the deterministic

limit, we expand $V(y)$ in Taylor series in $y - y_*$. Introducing $z = \varepsilon^{-1}(y - y_* - \Delta y_*)$, where Δy_* is a deterministic correction to y_* to be determined. Then, after a straightforward computation we obtain that to leading order $\Delta y_* = \varepsilon \ln \varepsilon^{-1} / |V'(y_*)|$, where $V' = dV/dy$, and the boundary layer solution $\rho_0(z)$ valid for $|z| \ll \varepsilon^{-1}$ is

$$\rho_0(z) = C \exp \left\{ - \frac{\nu(y_*)}{g(y_*)|V'(y_*)|} e^{|V'(y_*)|z} \right\}. \quad (16)$$

With $C=1$ this is also the probability that the trajectory has not jumped yet at $y = y_* + \Delta y_* + \varepsilon z$. Using this, we can compute the average jump-off point $\langle y \rangle$. Evaluating the necessary integrals, we finally obtain (to leading order in ε)

$$\langle y \rangle - y_* = \frac{\varepsilon}{|V'(y_*)|} \ln \left(\frac{g(y_*)|V'(y_*)|}{\varepsilon \nu(y_*) e^\gamma} \right), \quad (17)$$

where $\gamma \approx 0.5772$ is the Euler constant. Similarly, the standard deviation of the jump-off point is (to leading order)

$$\sqrt{\langle y^2 \rangle - \langle y \rangle^2} = \frac{\pi \varepsilon}{|V'(y_*)| \sqrt{6}}. \quad (18)$$

Note that the deterministic correction $\Delta y_* = \langle y \rangle - y_*$ contains a large logarithm and therefore always dominates the fluctuating contribution. Also, since the balance needed to obtain $\beta = O(1)$ implies that $\varepsilon = O(\ln \alpha^{-1})$, this, in turn, implies that $\Delta y_* = O(\ln \ln \alpha^{-1})$, and therefore gives a noticeable correction to y_* unless α is unrealistically small. We also point out that this results in the noticeable shift $\Delta T = \Delta y_* / g(y_*)$ of the period of the limit cycle.

We now check the validity of the picture presented above with KMC simulations of the Schnakenberg model. Figure 2 shows the results of a simulation for $\alpha = 10^{-4}$, $A = 0.5$, and $\varepsilon = 0.2$, a parameter set at which Eq. (9) has no limit cycle. This figure clearly shows a noise-induced coherent limit cycle due to SISR.⁸ Furthermore, by choosing parameters appropriately, we can make this motion more and more coherent. In Fig. 3 we plot the mean and standard deviation (as errorbars) of the jump-off point y [see Fig. 2(a)]. Here we take the parameters corresponding to $\beta = 1$, $A = 0.5$ and vary ε . Constraining the rate constants in this way and letting ε decrease, we can improve coherence of the SISR limit cycle. Note that the average jump-off point for the

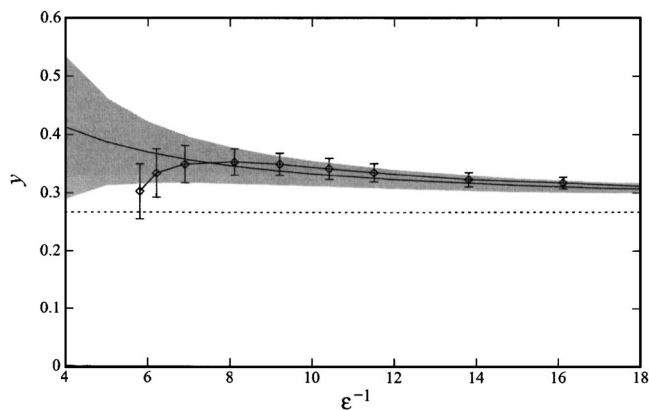


FIG. 3. Mean and standard deviation of the jump-off point y from the KMC simulations (data points) and theory (gray). The dotted line shows the value of y_* .

noise-induced limit cycle differs rather significantly from $y_* = 0.267$ predicted by the asymptotic theory due to the very slow convergence of the latter. However, including the fluctuation corrections from Eq. (17) results in excellent quantitative agreement between the simulation data and theory.

The effect of the intrinsic noise is demonstrated most dramatically by looking at the global bifurcation picture for the noise-induced limit cycle. In the absence of the noise the limit cycle appears via a Hopf bifurcation at $A = 1 + O(\alpha)$, and in the limit $\alpha \rightarrow 0$ appears in a discontinuous fashion at $A = 1$ (solid line in Fig. 4). The noise changes this qualitatively. In Fig. 4 we plotted the average frequency of the limit cycle

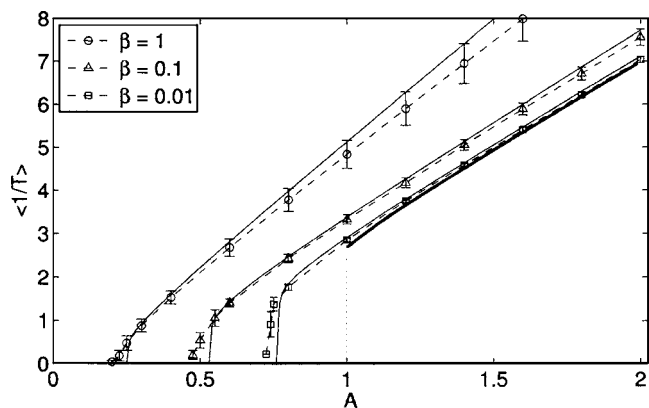


FIG. 4. Bifurcation diagram for the noise-induced limit cycle. Points are results of the simulations with $\alpha = 10^{-5}$, thin lines are theoretical predictions for the corresponding values of β . The thick line is the bifurcation diagram in the absence of the noise in the limit $\alpha \rightarrow 0$.

from the simulations for several values of β with $\alpha = 10^{-5}$ fixed. The period of the limit cycle shows $O(1)$ deviation from the meanfield behavior (solid line) for *all* values of A . The nature of the bifurcation is also altered. It is now creating an infinite period orbit. This is consistent with our theoretical prediction that (asymptotically) the limit cycle is born at $A = A_c < 1$, where A_c solves $\beta = \beta_c(A)$. The predicted limit cycle period also shows excellent agreement with theory in Fig. 4 (thin lines).

In conclusion, we have demonstrated that intrinsic fluctuations in systems far from equilibrium possessing fast/slow dynamics can have a profound effect on the observed dynamics, producing strongly non-meanfield, yet essentially deterministic dynamical behaviors.

The authors acknowledge partial support by NIH Grant No. R01 GM076690 (C.B.M), NSF Grant No. DMS02-09959, NSF Grant No. DMS02-39625, and ONR Grant No. N00014-04-1-0565 (E.V.-E.). This work was performed while E.V.-E. was visiting U.C. Berkeley as a Visiting Miller Research Professor.

¹E. M. Lifshits and L. P. Pitaevskii, *Physical Kinetics* (Pergamon Press, Oxford, 1981).

²C. W. Gardiner, *Handbook of Stochastic Methods* (Springer-Verlag, Berlin, 1985).

³A. Shwartz and A. Weiss, *Large Deviations for Performance Analysis* (Chapman and Hall, London, 1995).

⁴A. S. Pikovsky and J. Kurths, *Phys. Rev. Lett.* **78**, 775 (1997).

⁵B. Lindner, J. Garcia-Ojalvo, A. Neiman, and L. Schimansky-Geier, *Phys. Rep.* **392**, 321 (2004).

⁶M. I. Freidlin, *Stochastics Dyn.* **1**, 261 (2001).

⁷M. I. Freidlin, *J. Stat. Phys.* **103**, 283 (2001).

⁸C. B. Muratov, E. Vanden Eijnden, and W. E. Physica D **210**, 227 (2005).

⁹R. E. L. DeVille, E. Vanden Eijnden, and C. B. Muratov, *Phys. Rev. E* **72**, 031105 (2005).

¹⁰M. I. Freidlin and A. D. Wentzell, *Random Perturbations of Dynamical Systems* (Springer, New York, 1984).

¹¹P. Hänggi, P. Talkner, and M. Borkovec, *Rev. Mod. Phys.* **62**, 251 (1990).

¹²T. Wellens, V. Shatokhin, and A. Buchleitner, *Rep. Prog. Phys.* **67**, 45 (2004).

¹³D. T. Gillespie, *J. Comput. Phys.* **22**, 403 (1976).

¹⁴D. T. Gillespie, *J. Stat. Phys.* **16**, 311 (1977).

¹⁵J. Schnakenberg, *Rev. Mod. Phys.* **48**, 571 (1976).

¹⁶J. A. White, J. T. Rubinstein, and A. R. Kay, *Trends Neurosci.* **23**, 131 (2000).

¹⁷J. M. G. Vilar, H. Y. Kueh, N. Barkai, and S. Leibler, *Proc. Natl. Acad. Sci. U.S.A.* **99**, 5988 (2002).

¹⁸J. Paulsson, *Nature (London)* **427**, 415 (2004).

¹⁹J. Schnakenberg, *J. Theor. Biol.* **81**, 389 (1979).

²⁰A. Goldbeter, *Biochemical Oscillations and Cellular Rhythms* (Cambridge Univ. Press, Cambridge, 1996).

²¹R. E. L. DeVille, C. B. Muratov, and E. Vanden Eijnden (in preparation).